# Preparation and Characterization of Highly Oriented Poly(γ-benzyl L-glutamate) Networks and Gels with Long Channels with Micrometer-Scale Diameters

**Yuji Yamane, Masahito Kanekiyo, Satoshi Koizumi, Chenhua Zhao,* Shigeki Kuroki, Isao Ando**

*International Research Center of Macromolecular Science, Department of Chemistry and Materials Science, Tokyo Institute of Technology, 2-12-1 Ookayama, Meguro-ku, Tokyo 152-8552 Japan*

Received 23 August 2003; accepted 4 November 2003

**ABSTRACT:** Poly(γ-benzyl L-glutamate) (PBLG) gels with highly oriented α-helix chains were prepared by the crosslinking of PBLG chains through changes in the concentration of ethylenediamine, used as a crosslinker, in 1,4-dioxane in the presence of the strong magnetic field of an NMR magnet with a strength of 10.5 T. The experimental results showed that in one of these gels, long channels with an average diameter of about 100 μm were formed by phase separation between crosslinked PBLG and the solvent. Furthermore, three-dimensional $^1$H-NMR imaging patterns showed that the long channels were aligned in the direction parallel to the α-helix axis. The PBLG gel was swollen in the direction perpendicular to the α-helix axis, but it was not swollen in the direction parallel to the α-helix axis. The X-ray diffraction patterns of the gel showed that the interchain distance between the two nearest neighboring PBLG chains changed from 13.4 to 18.1 Å with a change in the swelling degree. © 2004 Wiley Periodicals, Inc. J Appl Polym Sci 92: 1053–1060, 2004

**Key words:** gels; networks; NMR; imaging; phase separation

## INTRODUCTION

Poly(γ-benzyl L-glutamate) (PBLG) forms a lyotropic liquid-crystalline phase in good solvents such as dichloromethane, 1,4-dioxane, and chloroform,[1–3] and it exhibits a sol–gel transition in *N*,*N*-dimethylformamide and benzyl alcohol.[4–7] The PBLG chains in the lyotropic liquid-crystalline phase are highly oriented in a magnetic field.[8–13] Kishi et al.[14,15] prepared PBLG gels in cholesteric and nematic liquid-crystalline phases and then studied the properties of the obtained gels. In our previous works, it has been reported that a highly oriented PBLG gel can be prepared by the crosslinking reaction of highly oriented PBLG chains with a crosslinker in the magnetic field of an NMR magnet through the monitoring of the orientation of the PBLG chains with solid-state static $^{13}$C-NMR;[16] then, solvents and rodlike molecules in the PBLG gel anisotropically diffuse in the directions parallel and perpendicular to the α-helix axis by a high-field-gradient NMR system.[16–24] This shows that there exist long channels with small diameters of 15–20 Å in the highly oriented PBLG gel.

On the basis of this background, we believe that if we change the concentration of the crosslinker, we can control the diameter of long channels formed by highly oriented PBLG chains in the strong magnetic field of an NMR magnet. This is the motivation behind this work. Therefore, we prepared a PBLG gel with highly oriented α-helix chains by crosslinking chains by changing the concentration of ethylenediamine, used as a crosslinker, in a 1,4-dioxane solution placed in the strong magnetic field of an NMR magnet with a strength of 10.5 T. The properties of the highly oriented PBLG gel were characterized by wide-angle X-ray diffraction, optical microscopy, three-dimensional (3D) NMR imaging, and volume swelling measurements.

## EXPERIMENTAL

### Materials and gel preparation

PBLG (weight-average molecular weight = 277,000) was kindly supplied by Ajinomoto Co., Ltd. (Tokyo,

*Correspondence to:* I. Ando (iando@polymer.titech.ac.jp).
**Present address:* Protein Research Group, Riken Genomic Sciences Center, 1-7-22 Suehiro-cho, Tsurumi-ku, Yokohama, Kanagawa, 230-0045 Japan.

Contract grant sponsor: Japanese Ministry of Education, Culture, Sports, Science, and Technology (through Special Coordination Funds and a Grant-in-Aid for Promoting Science and Technology).

Contract grant sponsor: New Energy and Industrial Technology Development Organization (through the 2001 Nanostructure Polymer Project).

Journal of Applied Polymer Science, Vol. 92, 1053–1060 (2004)

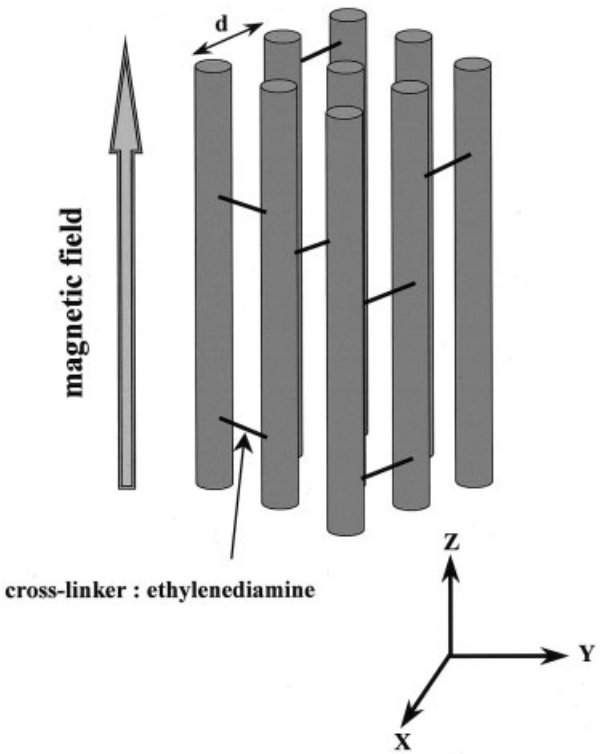


**Figure 1** Schematic 3D structure of a highly oriented PBLG network. *d* is the interchain distance between two nearest neighboring PBLG chains.

Japan). A 25 wt % lyotropic, liquid-crystalline PBLG solution was prepared with 1,4-dioxane as a solvent. A PBLG solution (0.2 g) in a Teflon tube with a diameter of 5 mm was placed in the strong magnetic field of an NMR magnet (10.5 T) for 24 h at room temperature to highly orient the $\alpha$-helix PBLG chains in the magnetic field direction, for which an orientation degree of about 0.81 was reported previously. After the Teflon tube with highly oriented PBLG chains was removed from the NMR magnet, ethylenediamine as a crosslinker was added through changes in the concentration in the tube (sample A, 5 $\mu$L sample B, 10 $\mu$L; and sample C, 20 $\mu$L). The sample tube was placed for 3 days in an NMR magnet, again, at room temperature, and this led to crosslinking of the PBLG chains in the lyotropic liquid-crystalline phase by an ester–amide exchange reaction. The obtained highly oriented PBLG samples, A–C, were washed with 1,4-dioxane for the removal of unreacted crosslinker. The dried samples were opaque, cylindrical rods with average diameters of 2 mm and lengths of 15 mm.

Optical microscopy observations of the highly oriented PBLG gels were made with an Olympus CH-2 microscope (Tokyo, Japan) at room temperature. These observations showed that the gels were highly oriented (Fig. 1).

### Measurements

#### NMR imaging measurements

All the $^1$H-NMR image patterns of the highly oriented PBLG gels were observed with a Bruker DSX-300 spectrometer (Karlsruhe, Germany) operating at 300 MHz with an imaging system with a maximal gradient strength of 100 mT/m at room temperature. The two-dimensional (2D) imaging method has the disadvantage of a relatively low signal-to-noise ratio and reduced slice coverage in comparison with the 3D NMR imaging method, although the measurement time is very short. 3D NMR imaging provides a clear 3D structure of a sample, and volume acquisition provides a high signal-to-noise ratio and minimal effective slice thickness.[25–27] Thus, for the analysis of the 3D structure of the channels in the PBLG gels, the imaging pulse sequence was based on the 3D gradient echo (GE) pulse sequence (Fig. 2).[28,29] Data processing of the 3D images was performed by the 3D Fourier transform method. For the acquisition and processing of the NMR data, Para Vision programs supplied by Bruker were used. In the 3D GE method, the field gradients in the $y$ and $z$ directions ($G_z$ and $G_y$, respectively) are phase-encoding gradients, whereas the field gradient in the $x$ direction ($G_x$) is the frequency-encoding gradient. The 3D NMR image patterns were produced by a 3D GE pulse sequence with the following parameters: the flip angle was 30°, the repetition time was 1 s, and the echo time was 20 ms. The field of view was 10.8 mm $\times$ 10.8 mm $\times$ 2.7 mm, the data points were 256 $\times$ 256 $\times$ 32, and the voxel size was 42 $\mu$m $\times$ 42 $\mu$m $\times$ 84 $\mu$m.

#### Wide-angle X-ray diffraction measurements

Wide-angle X-ray diffraction patterns of PBLG gel samples and dried samples were recorded with a flat-plate camera mounted onto a Rigaku-Denki X-ray generator (Tokyo, Japan) with Ni-filtered Cu K$\alpha$ radiation. All the experiments were performed at room temperature (ca. 20°C). From the obtained X-ray diffraction patterns, the interchain distances between the two nearest neighboring PBLG chains were determined.

## RESULTS AND DISCUSSION

### Swelling properties of the highly oriented PBLG gels

Dried samples A and B were opaque, cylindrical rods with an average diameter of 2 mm and a length of 15 mm, and they were swollen to equilibrium by 1,4-dioxane. Dried sample C was not swollen by 1,4-dioxane. The density of crosslinking in sample C was very high because it was crosslinked at a high concentration of the crosslinker ethylenediamine. As a result,

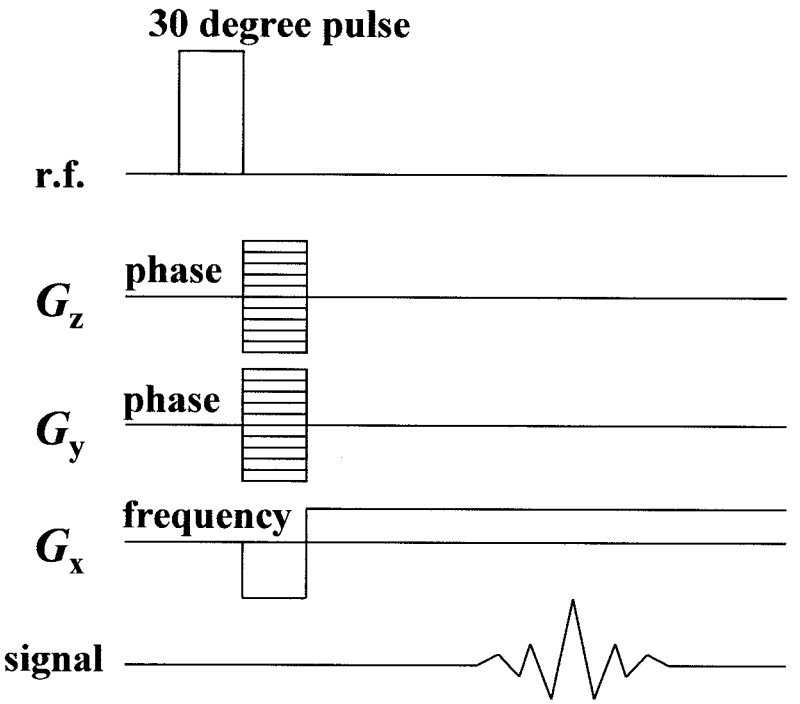


**Figure 2** 3D GE pulse sequence.

1,4-dioxane molecules did not diffuse into the PBLG network.

The swelling ratios of the lengths for the *X*, *Y*, and *Z* directions of the cylindrical PBLG gel samples, in equilibrium to those for the corresponding dried rod samples, were measured with a microscope, and they are shown in Table I. The *Z* direction of the cylindrical gel was along the cylindrical axis, which was in the direction parallel to the α-helix axis, and the *X* and *Y* directions of the cylindrical gel were perpendicular to the cylindrical axis, which was in the direction perpendicular to the α-helix axis. For sample A, the swelling ratios for the *X*, *Y*, and *Z* directions ($Q_X$, $Q_Y$, and $Q_Z$) were 1.44, 1.74, and 1.11, respectively. The cross section of the swollen rod sample was not circular. The degree of volume swelling ($Q_{XYZ} = Q_X \times Q_Y \times Q_Z$) was estimated to be 2.79. These experimental results showed that the swelling was anisotropic, that almost no swelling occurred in the direction parallel to the α-helix axis, but swelling did largely occur in the direction perpendicular to the α-helix axis, and that the immersion of 1,4-dioxane as a solvent led to an

**TABLE I**
**Preparation Conditions and Properties of Highly Oriented PBLG Gels**

| | PBLG (g) | 1,4-Dioxane (g) | Ethylenediamine (μL) | Swelling ratios in the *x*, *y*, and *z* directions[a] | | Volume swelling ratio[a] | Interchain distance between the two nearest neighboring PBLG chains/(Å)[b] | |
|---|---|---|---|---|---|---|---|---|
| | | | | *x* | 1.44 | | | |
| A | 0.05 | 0.15 | 5 | *y* | 1.74 | 2.79 | Dry | 13.4 |
| | | | | *z* | 1.11 | | Gel | 21.2 |
| | | | | *x* | 1.50 | | | |
| B | 0.05 | 0.15 | 10 | *y* | 1.75 | 2.62 | Gel | 18.1 |
| | | | | *z* | 1.00 | | | |
| C | 0.05 | 0.15 | 20 | No swelling | | | | |

[a] With respect to to the dried state. The *z* direction and the *x* and *y* directions were parallel and perpendicular, respectively, to a cylindrical PBLG gel.
[b] As determined by X-ray diffraction.

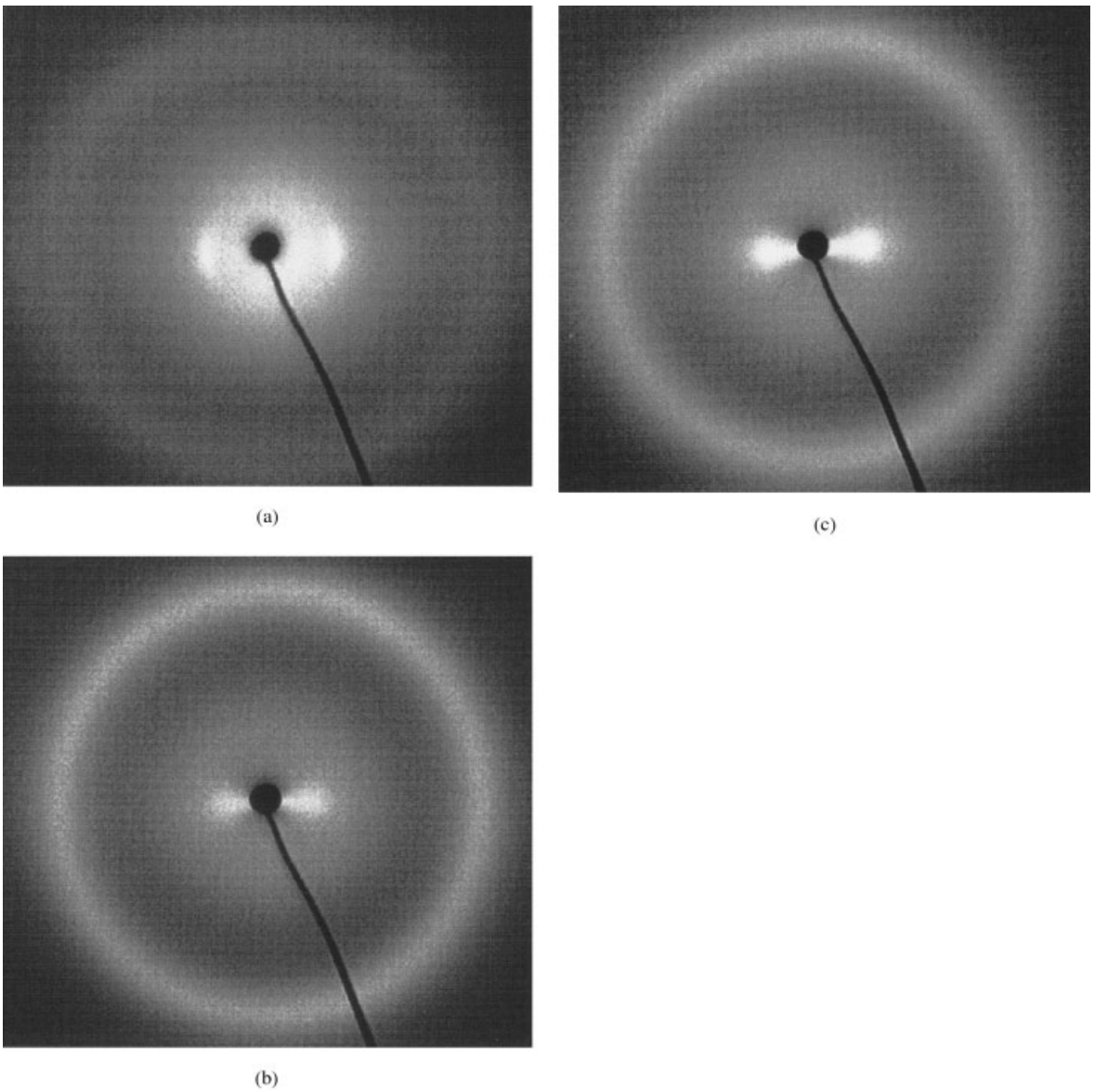


**Figure 3** X-ray diffraction patterns of highly oriented PBLG networks and gels with 1,4-dioxane: (a) sample A in the dry state, (b) sample A in the gel state, and (c) sample B in the gel state.

increase in the PBLG interchain distance through the high orientation of the PBLG chains. For sample B, the swelling ratios for $Q_X$, $Q_Y$, and $Q_Z$ were 1.50, 1.75, and 1.00, respectively. The cross section of the swollen rodlike sample was not circular. $Q_{XYZ}$ was estimated to be 2.62. The swelling was anisotropic, like that of sample A. As shown by the crosslinker concentration used to prepare samples A and B, the density of crosslinking for sample B was higher than that for sample A. Thus, as previously described, the swelling ratios for sample B were smaller than those for sample A.

### PBLG interchain distance in the gel state and dried state

Wide-angle X-ray diffraction patterns were obtained for PBLG gels with highly oriented chains and their dried samples for the analysis of the molecular packing of PBLG chains in the dried state and in the gel state. Figure 3(a,b) shows photographs of X-ray diffraction patterns for the dried state and the gel state of sample A, respectively. From the X-ray diffraction pattern of the PBLG network, the interchain distances between the two nearest neighboring PBLG chains for the dried state and the gel state were determined to be 13.4 and 21.2 Å, respectively. This showed that the interchain distance in the gel state became larger than that in the dried state, as expected. The swelling ratio ($Q_{XY} = Q_X \times Q_Y$) obtained by microscopy was 2.50, and the swelling ratio $Q_{XY}$ determined by wide-angle X-ray diffraction was 2.49; they agreed with each other. However, for the sample B gel [Fig. 3(c)], the interchain distance between the two nearest neighbor-

ing PBLG chains was 18.1 Å. This value was much smaller than that of sample A, as expected because the density of crosslinking for sample B was higher than that for sample A.

### Observation of the cross sections of highly oriented cylindrical PBLG networks by optical microscopy

The cross sections of highly oriented cylindrical PBLG networks (samples A and B) were studied by optical microscopy, and their photographs are shown in Figure 4. Figure 4(b) shows that there existed many channels, with circular cross sections with a micrometer-scale diameter, in the direction parallel to the cylindrical axis, that is, in the direction parallel to the PBLG $\alpha$-helix axis. This was also shown by 3D $^1$H-NMR imaging patterns (discussed later). However, for sample A, the existence of channels with circular cross sections with a micrometer-scale diameter cannot be recognized, as shown in Figure 4(a). Therefore, it can be said that channels with circular cross sections with a micrometer-scale diameter appeared in the highly oriented PBLG network with a high density of crosslinking.

### $^1$H-NMR imaging analysis of the highly oriented cylindrical PBLG gels

3D NMR imaging patterns of a cylindrical and highly oriented PBLG gel (sample B) with long channels were studied to determine whether the long channels were formed in the direction parallel to the cylindrical axis through the whole sample or not. The PBLG gel sample B, swollen with 1,4-dioxane, was placed in an NMR tube with a diameter of 5 mm. The observed 3D $^1$H spin density NMR image patterns of this sample are shown in Figure 5. Thirty-two pieces of the *XY*-plane-sliced images were observed with a thickness of 84 $\mu$m per image in the *Z* direction, and 12 pieces (slice 1 is the upside of the sample and slice 12 is the downside of the sample) are shown. In these images, there are many white, circular regions in the background. This shows that the signal intensity of the solvent in the channels was very intense, but that of the solvent in the PBLG network was very weak, because the density of the solvent in the channel was much higher than that in the network. Therefore, it can be said that the white, circular regions came from 1,4-dioxane as a solvent in long channels with a micrometer-scale diameter in the PBLG sample, and the black region indicates the PBLG network with the solvent.

If we look at the image patterns carefully, we can see that the positions of the white, circular regions are the same in every image pattern. This means that the long channels were formed in the direction parallel to the cylindrical axis through the whole sample as circular channels. Furthermore, there were no long channels with a micrometer-scale diameter until about 500 $\mu$m from the outside surface of the gel rod.

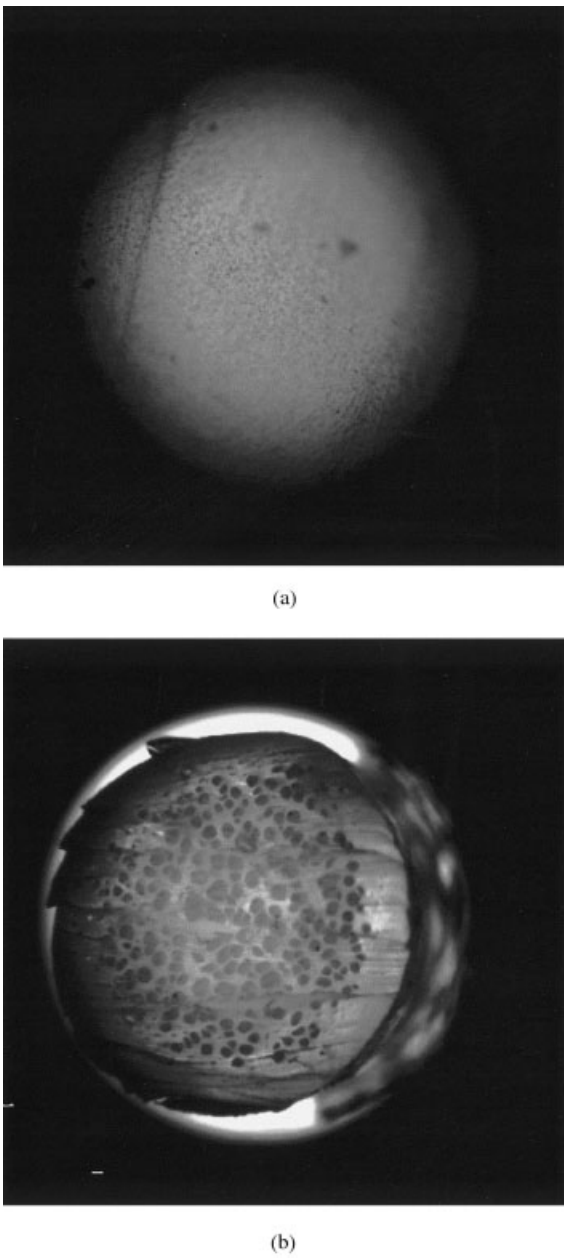


**Figure 4** Optical microscopy photographs of highly oriented PBLG networks: (a) sample A in the dry state and (b) sample B in the dry state.

Furthermore, if we look at the white, circular regions carefully, we can see that the diameter of the white, circular regions was not homogeneous. Therefore, the distribution of the diameter sizes in the gel sample was analyzed with a 2D slice image taken from 3D NMR image data sets. The plots of the number of the white, circular regions against the diameter size are shown in Figure 6, in which the shape of the white region is roughly a circle. Most of the diameters were 49–139 $\mu$m, and the average was

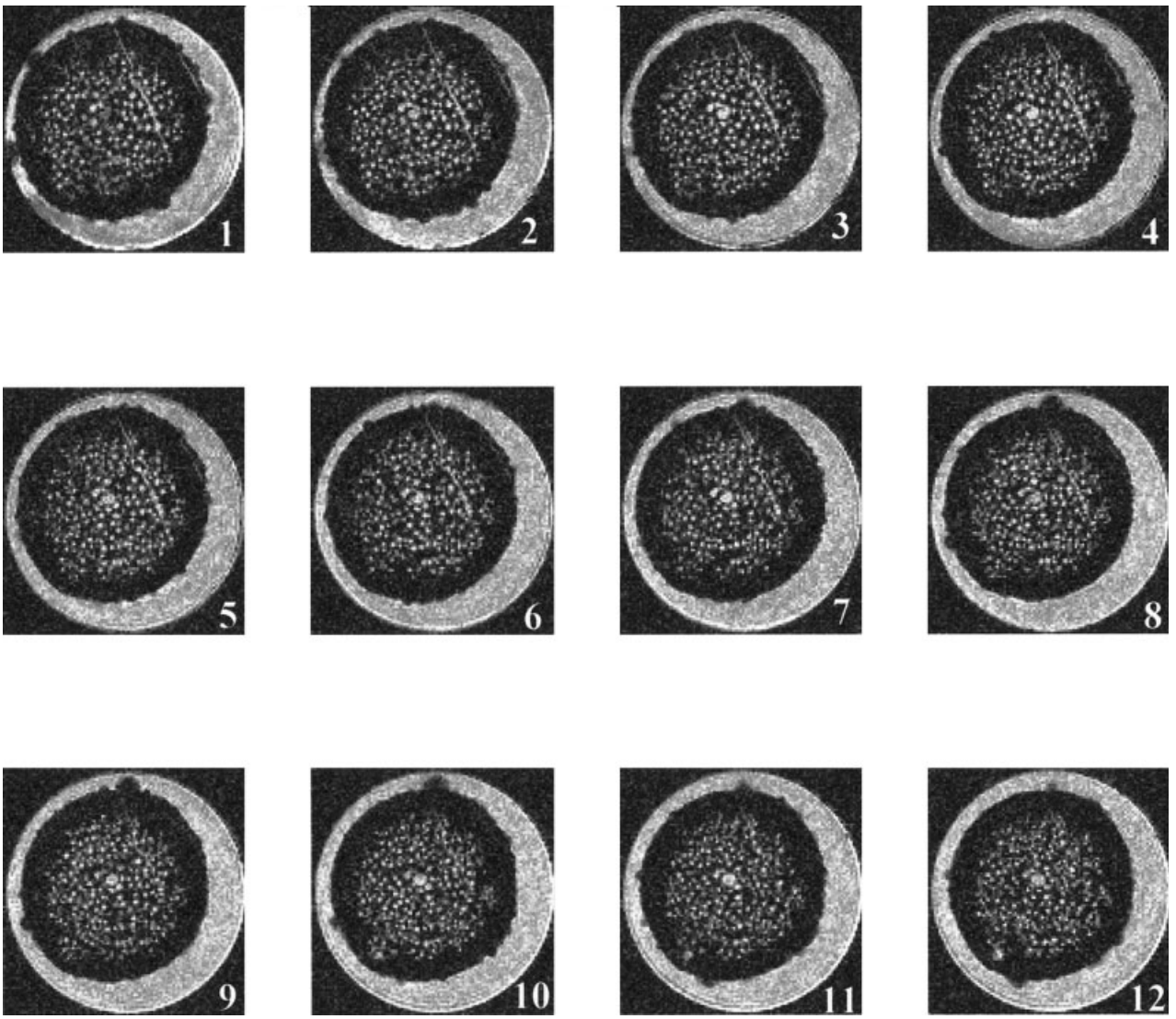


**Figure 5** 2D $^1$H spin density NMR image patterns of a highly oriented PBLG gel (sample B) with 1,4-dioxane as a solvent. Thirty-two pieces of *XY*-plane-sliced images were observed, each image being 84 $\mu$m thick in the *Z* direction; 12 pieces are shown. Slice 1 is the upside of the sample, and slice 12 is the downside of the sample; the interval thickness was 84 $\mu$m. The 2D image slices were taken from 3D NMR image data sets of sample B.

98.9 $\mu$m. For convenience, a schematic diagram of a rodlike and highly oriented PBLG gel with long channels is shown in Figure 7. Figure 7 suggests large channels toward the center of the rodlike gel.

Next, we are concerned with the origin of the formation of long channels with circular cross sections with a micrometer-scale diameter in a highly oriented PBLG gel prepared by crosslinking in a strong magnetic field. However, clarifying the origin of the formation of long channels in a gel is not simple. Nevertheless, it seems that this is similar to a phase-separation phenomenon. On the basis of this consideration, we assume that with an increase in the crosslinking of highly oriented PBLG chains in a solvent, in which originally the chains have a large interchain distance because of sufficient solvent between them, the solvent must be discharged and phase separation then occurs. This consideration may be not far from the origin of the formation of the long channels in the highly oriented PBLG gel. It is known that a PBLG solution sometimes exhibits phase separation under a specified condition. For example, as proposed by Miller and coworkers,[30,31] phase separation is an important factor in the formation of physically crosslinking PBLG gels. The thermoreversible gelation of rodlike polymers such as PBLG also occurs sometimes.[32,33]

Furthermore, we prefer to say that highly oriented PBLG gels with long channels with a micrometer-scale diameter in the direction parallel to the orien-

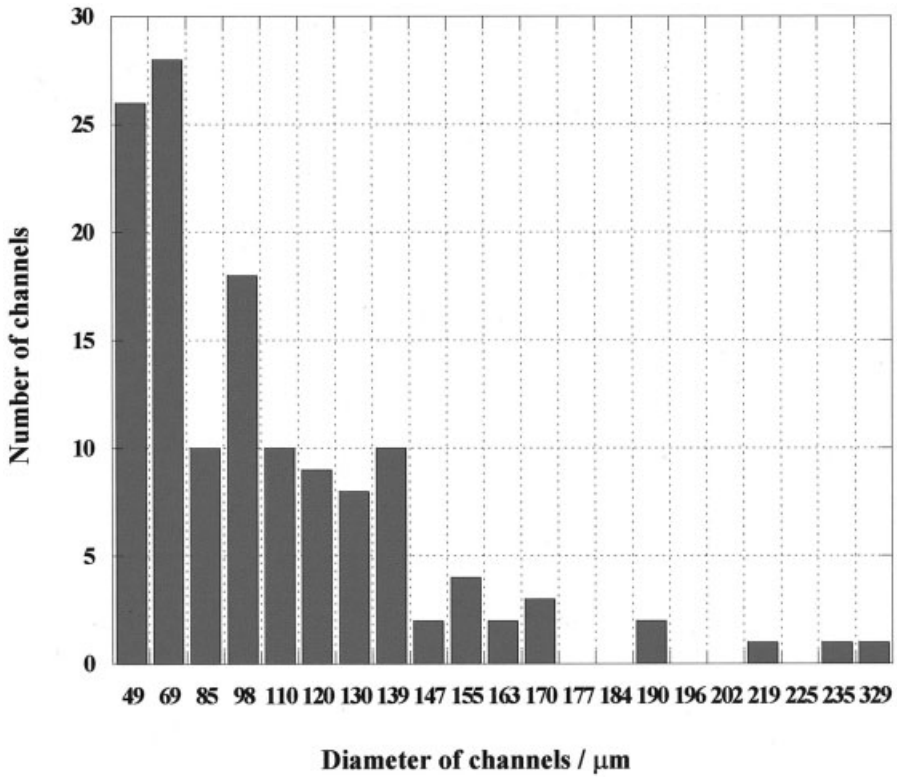


**Figure 6** Plots of the number of the white, circular regions of a highly oriented PBLG gel (sample B) with 1,4-dioxane in a 2D slice image taken from 3D NMR image data sets against the diameter size.

tation axis may have potential as biomaterials with channels with special active fields. At present, we are developing highly oriented PBLG gels with long channels with a nanoscale diameter in the direction parallel to the orientation axis with this technique.

Finally, we conclude that PBLG gels with long channels with an average diameter of about 100 μm were prepared and characterized.

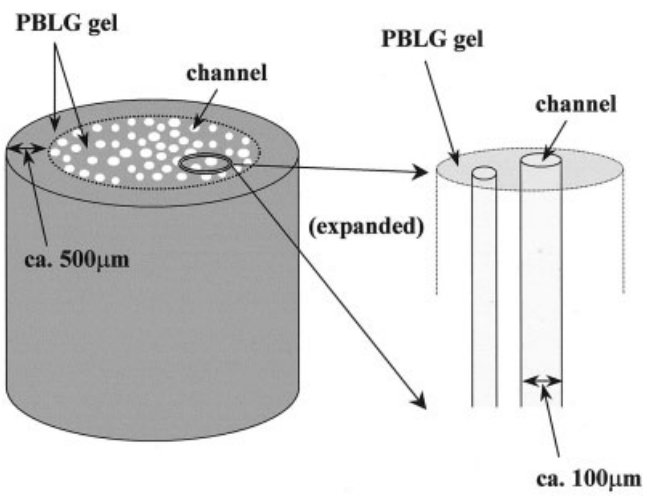


**Figure 7** Schematic diagram of a highly oriented, rodlike PBLG gel with long channels.

## References

1. Robinson, C. Trans Faraday Soc 1956, 52, 571.
2. Robinson, C.; Ward, J. C. Nature 1957, 189, 1183.
3. Robinson, C. Tetrahedron 1961, 13, 219.
4. Sasaki, S.; Tokuma, K.; Uematsu, I. Polym Bull 1983, 10, 539.
5. Ginzburg, B.; Siromyatnikova, T.; Frenkel, S. Polym Bull 1985, 13, 139.
6. Cohen, Y.; Dagan, A. Macromolecules 1995, 28, 7638.
7. Dadmun, M. D.; Muthukumar, M.; Schwahn, D.; Springer, T. Macromolecules 1996, 29, 207.
8. Sobajima, S. J Phys Soc Jpn 1967, 23, 1070.
9. Panar, M.; Phillips, W. D. J Am Chem Soc 1968, 90, 3859.
10. Orwell, R. D.; Vold, R. L. J Am Chem Soc 1971, 93, 5335.
11. Samulski, E. T.; Tobolsky, A. V. Mol Cryst Liq Cryst 1969, 7, 433.
12. Fung, B. M.; Gerace, M. J.; Gerace, L. S. J Phys Chem 1983, 74, 83.
13. Ando, I.; Hirai, T.; Fujii, Y.; Nishioka, A.; Shoji, A. Macromol Chem 1983, 184, 2592.
14. Kishi, R.; Sisido, M.; Tazuke, S. Macromolecules 1990, 23, 3779.
15. Kishi, R.; Sisido, M.; Tazuke, S. Macromolecules 1990, 23, 3868.
16. Zhao, C.; Zhang, H.; Yamanobe, T.; Kuroki, S.; Ando, I. Macromolecules 1999, 32, 3389.
17. Zhao, C.; Kuroki, S.; Ando, I. Macromolecules 2000, 33, 4486.
18. Yamane, Y.; Kobayashi, M.; Kuroki, S.; Ando, I. Macromolecules 2001, 34, 5961.
19. Yin, Y.; Zhao, C.; Kuroki, S.; Ando, I. Macromolecules 2002, 35, 2335.
20. Yamane, Y.; Kobayashi, M.; Kimura, H.; Kuroki, S.; Ando, I. Polymer 2002, 43, 1767.
21. Yin, Y.; Zhao, C.; Sasaki, A.; Kimura, H.; Kuroki, S.; Ando, I. Macromolecules 2002, 35, 5910.
22. Kim, S.; Kimura, H.; Kuroki, S.; Ando, I. Chem Phys Lett 2003, 367, 581.

23. Yamane, Y.; Matsui, M.; Kimura, H.; Kuroki, S.; Ando, I. J Appl Polym Sci 2003, 89, 413.
24. Yamane, Y.; Matsui, M.; Kimura, H.; Kuroki, S.; Ando, I. Macromolecules 2003, 36, 5655.
25. Brandt-Zavadzki, M. N.; Gillan, G. D.; Atkinson, D. J.; Edalatpour, N.; Jensen, M. J Magn Reson Imaging 1993, 3, 656.
26. Runge, V. M.; Kirsch, J. E.; Thomas, G. S.; Mugler, J. P. J Magn Reson Imaging 1991, 1,493.
27. Hasse, A.; Frahm, J.; Matthaei, D.; Hänicke, W.; Merboldt, K. D. J Magn Reson 1986, 67, 258.
28. Callaghan, T. P. Principles of Nuclear Magnetic Resonance Microscopy; Clarendon: Oxford, 1991.
29. Tohyama, K.; Miller, W. G. Nature 1981, 289, 813.
30. Miller, W. G.; Russo, P. S.; Chakrabarti, S. J Appl Polym Sci Appl Polym Symp 1985, 41,49.
31. Schmidkte, S.; Russo, P. S.; Nakamatsu, J.; Buyuktanir, E.; Turfan, B.; Temyanko, E. Macromolecules 2000, 33, 4427.
32. Tanaka, F. Macromolecules 2000, 33, 4249.
33. Oikawa, H.; Nakanishi, H. J Chem Phys 2001, 115, 3785.